A Highly Photoconductive Poly(vinylcarbazole)/2,4,7-Trinitro-9-fluorenone Sol–Gel Material that Follows a Classical Charge-Generation Model

ARTICLE *in* THE JOURNAL OF PHYSICAL CHEMISTRY B · JANUARY 2007

Impact Factor: 3.3 · DOI: 10.1021/jp0629184 · Source: PubMed

3 AUTHORS:

G. Ramos
Instituto Nacional de Técnica Aeroespacial
39 PUBLICATIONS **241** CITATIONS
SEE PROFILE

Tomas Belenguer
Instituto Nacional de Técnica Aeroespacial
106 PUBLICATIONS **582** CITATIONS
SEE PROFILE

David Levy
Spanish National Research Council
128 PUBLICATIONS **3,728** CITATIONS
SEE PROFILE

A Highly Photoconductive Poly(vinylcarbazole)/2,4,7-Trinitro-9-fluorenone Sol−Gel Material that Follows a Classical Charge-Generation Model

Gonzalo Ramos,*,†,‡ Tomás Belenguer,† and David Levy*,†,‡

Instituto Nacional de Técnica Aeroespacial-INTA, Laboratorio de Instrumentación Espacial-LINES, Torrejón de Ardoz, 28850, Madrid, Spain, and Instituto de Ciencia de Materiales de Madrid-ICMM, Consejo Superior de Investigaciones Científicas-CSIC, Cantoblanco, 28049, Madrid, Spain

Received: May 12, 2006; In Final Form: September 28, 2006

Highly photoconductive properties are reported for organic−inorganic hybrid sol−gel thin film materials composed of a classical poly(vinylcarbazole)/2,4,7-trinitro-9-fluorenone (PVK/TNF) polymeric mixture, entrapped in a SiO_2 matrix, whose pores have been chemically modified by organic functional groups. The highest photosensitivity obtained, 3.4×10^{-10} cm Ω^{-1} W^{-1} at $E \approx 22$ V μm^{-1}, at the optimum molar ratio between the active components, TNF, PVK, and SiO_2, is in the range of the highest values ever reported for any PVK/TNF-based classical photoconductive material. It is demonstrated that the PVK/TNF-based sol−gel films follow Onsager's classical charge-generation model. The analysis of the photocurrent efficiency (Φ) of PVK/TNF-based sol−gel films by such a model provides the primary quantum yield of thermalized pair formation and the initial thermalized pair distance, $\phi_0 = 0.12$ and $r_0 = 66.1$ Å, respectively, for the optimized sample. As a result of Onsager's analysis, a notorious improvement of the photocurrent generation process was achieved for low TNF concentrations.

1. Introduction

Photoconductivity in organic materials, which is wavelength, electric field, and temperature dependent, consists of two processes: photogeneration of charge carriers and their subsequent transport.[1] Usually, low photogeneration efficiencies were ascribed to the initial recombination of a photoinduced electron and its parent cation. These geminate recombinations are frequently produced in organic materials due to their low relative permittivity (low coulomb attraction screening).[2] In the late 1960s, Batt et al.[3] described a model of geminate recombination, based on Onsager's theory,[4] that involved the field-assisted thermal dissociation of a charge-transfer state.[5,6] Since then, Onsager's theory, which provides a more detailed description of the photoconductive behavior in materials, has been widely employed to describe the photogeneration of free charge carriers in various photoconductive materials, such as molecularly doped polymers,[5] pure polymers,[5,7] amorphous semiconductors,[8] and molecular aggregates.[5,6]

Organic photoconductive materials have attracted a great deal of attention during the last three decades, as can be appreciated by their involvement in different interesting fields such as xerography (both classical and holographic)[9−11] and photorefractivity.[12−18] In addition to its thermoplastic behavior in holographic xerography applications or optical nonlinearity in photorefractivity, photoconductivity is a required property that will determine the optimum performance of the material. Photoconductivity has been observed in a variety of polymers, whether doped with organic or inorganic entities that may act as charge-transfer complexes.[1,9,12,13,19,20] Among them, poly(vinylcarbazole)/2,4,7-trinitro-9-fluorenone (PVK/TNF)-based classical composites have been widely explored, due of the good performance of PVK as a charge-transporting matrix (hole transporting) and of TNF as a sensitizer.[11−13,17,21−25] The photoconductivity in PVK/TNF-based composites results from the formation of a charge-transfer complex between the TNF and the carbazole units in the PVK.[17−26] To optimize the photoconductivity in a PVK/TNF-based material a careful balance between the components is required as well as a high photogeneration and transport.[27]

The sol−gel approach appears as a very promising route for the preparation of photoconductive materials.[1,28−30] The mild synthesis conditions offered by the sol−gel route (process begins at the solution stage and takes place at room temperature) allow the incorporation of the optically active organic molecules within the porosity of the resulting amorphous matrix. Thus, photoconductive sol−gel materials can be prepared by mimicking the classical polymeric materials, with the advantage that using silica gel instead of a polymer matrix as the supporting material will provide better stability and higher optical quality.[28,29] During the last years, photoconductive sol−gel materials have been mainly obtained through the incorporation of dispersed carbazole units within the porosity of the silica matrix, whether covalently bonded to the silica network or not, e.g., carbazole functionalized sol−gel precursor[1,28] or ethylcarbazole,[30] respectively. The photosensitivity values found in sol−gel materials were similar or higher than those obtained for PVK/TNF-based classical photoconductive polymers, pointing out the unnecessary use of massive PVK as host polymeric matrix.[31]

The aim of this work is to find an optimal preparation procedure and the characterization of organic−inorganic hybrid sol−gel thin films based on a classical PVK/TNF polymeric mixture entrapped into the porosity of a SiO_2 matrix, whose pores have been chemically modified by organic functional groups. The optimization of the PVK/TNF-based sol−gel material was carried out to maximize its photoresponsive

* Address correspondence to these authors. G.R.: phone +34-91-5201913, fax +34-91-5201317, e-mail ramoszg@inta.es. D.L.: phone +34-91-3349076, fax +34-91-3720623, e-mail d.levy@icmm.csic.es.

† Instituto Nacional de Técnica Aeroespacial-INTA.

‡ Instituto de Ciencia de Materiales de Madrid-ICMM.

10.1021/jp0629184 CCC: $33.50
Published on Web 11/14/2006

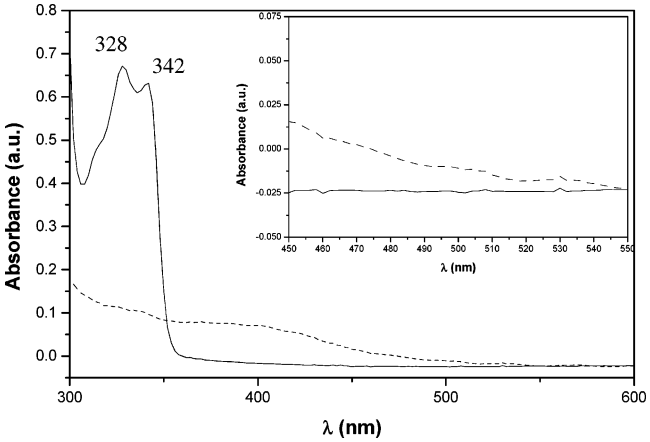

Figure 1. Absorption spectra of a PVK/TNF-based sol−gel material before (dash line) and after 2 h of UV illumination (solid line). In the inset, the extension of the spectrum for larger wavelengths is depicted.

performance by means of adjusting the TNF/PVK and PVK/SiO_2 molar ratios in the film. Once demonstrated that the PVK/TNF-based sol−gel materials follow Onsager's classical charge-generation model, the resulting photocurrent efficiency (Φ) was analyzed to obtain the primary quantum yield, ϕ_0, and the initial thermalized pair distance, r_0, that allows establishing the relationship between both parameter's and the material's photoresponse evolution.

2. Materials and Methods

2.1. Film Preparation. Hybrid PVK/TNF-based sol−gel photoconductive materials were prepared by acid hydrolysis (water at pH 1, 11.0 mmol) of glycidoxypropyltrimethoxysilane (GPTMS, 5.5 mmol) under stirring. Once a clear and homogeneous sol is formed, a pyridine solution (0.9 mL, Aldrich) with the *N*-vinylcarbazole (NVC, Aldrich), 1,1-dimethoxy-1-phenylacetophenone (IRG-651, CYBA), and 2,4,7-trinitro-9-fluorenone (TNF, from Ultra Scientific) was added drop by drop under vigorous stirring. The sol was heated at 75 °C for 10 min before the addition of 25 μL of 2-(dibutylamino)ethanol (Aldrich). The resulting brownish sol was filtered (0.2 μm) and dip coated onto an indium tin oxide glass substrate (ITO) at a dipping rate of 15 cm/min. Films with a thickness of 8.0 ± 0.8 μm (Deck Tak III profilometer) were obtained. Samples were thermal treated at 50 °C overnight. The PVK network was obtained through the photopolymerization (UV illumination for 2 h with a ULTRA-VITALUX lamp) of the NVC caged within the porous silica matrix. PVK polymerization was monitored by the appearance of the peaks at 328 and 342 nm in the absorption spectra (Figure 1).[32,33] The resulting hybrid PVK/TNF-based sol−gel samples were codified as PVK(x)/TNF(y), where x and y stand for PVK/GPTMS and TNF/PVK molar ratio × 100, respectively. Counter electrodes were fabricated on the film surface by Ag painting (0.02 Ω cm^{-2} of surface resistance). Polyimide tape (Kapton, surface resistance: 10^{18}Ω cm^{-2}), with a thickness of 80 μm, located between the sample surface and the electrode, was used with a double function: first, to ensure the blocking nature of the electrode (and hence, to improve the photoconductive performance in dark conditions and under illumination by preventing the charge injection[5,34]), and second, to avoid the impregnation of the sol−gel matrix with the Ag paint.

2.2. Characterization. The photoconductive behavior of the material has been evaluated in terms of its photosensitivity (S_{ph} in eq 1), which is defined as the photoconductivity (σ_{ph}, photocurrent density per unit of applied electric field) normalized by the illumination irradiance (I):[12,28]

$$S_{ph} = \frac{J_{ph}}{EI} = \frac{\sigma_{ph}}{I} \tag{1}$$

where the photocurrent density (J_{ph}) is the light induced current component per unit of illuminated material area. The photocurrent measurements were carried out by using a simple DC photocurrent technique (PC).[2,12,31,35] Samples were left in the dark for at least 5 min before measurements, to obtain a stable dark current. An Ar^+ laser working at a wavelength of 514 nm was used as the excitation source, although it was demonstrated that the photoresponse of the PVK/TNF-based sol−gel material is more efficient at other wavelengths.[31] The photoinduced current was measured 60 s after turning the light on. The current with and without illumination was measured with a Keithley 615 electrometer. The current component induced by light excitation was determined by subtracting the dark current from the photocurrent. The experimental setup was carefully selected to avoid the undesirable combination effects; i.e., the irradiance of the excitation source was fixed at 8.5 mW cm^{-2} and the characterization was carried out under temperature- and pressure-controlled conditions (20 °C and normal pressure) to ensure that the variation of the S_{ph} values corresponds just to differences in the sample composition. For a complete characterization of the photoconductive material, the photocurrent efficiency was analyzed employing Onsager's charge generation model. The photocurrent efficiency (Φ in eq 2) is defined as the number of measured charge carriers per absorbed incident photon,[36]

$$\Phi = \frac{2hc}{e\lambda}\frac{J_{ph}}{\alpha dI} \tag{2}$$

where c is the light speed, λ is the wavelength of the incident radiation, h is Planck's constant, α is the absorption coefficient, and d is the sample thickness. Both α and d are included to take into account the sample absorption at the working wavelength. The averaged travel distance of the charge carriers generated in such a weakly absorbing sample were also considered.[36]

The photogeneration efficiency [$\Phi(r_0,E)$], being the product of the quantum yield of thermalized pair formation and the pair dissociation probability, is interpreted in terms of a two-step process. In the first step, a fraction of absorbed photons results in bound thermalized pairs (primary quantum yield, ϕ_0). In the second step, the bound thermalized pairs created can either recombine or separate to form a free electron and a free hole. In the presence of an electric field (E), and assuming that the initial spatial distribution of the interpair distance [$g(r,\theta)$, where θ is the polar angle] is an isotropic δ function [$g(r,\theta) = \delta(r - r_0)4^{-1}\pi^{-1}r_0^{-2}$],[5,6] $\Phi(r_0,E)$ is given by eq 3:

$$\Phi(r_0,E) = \phi_0\left[1 - \frac{1}{2\xi}\sum_{j=0}^{\infty}A_j(\eta)A_j(2\xi)\right] \tag{3}$$

where

$$A_{j+1}(\eta) = A_j(\eta) - \frac{\eta^{j+1}e^{-\eta}}{(j+1)!} \tag{4}$$

$$A_0(\eta) = 1 - e^{-\eta} \tag{5}$$

$$\eta = \frac{e^2}{\epsilon kTr_0} \tag{6}$$

$$2\xi = \frac{eEr_0}{kT} \tag{7}$$

and r_0 is the initial thermalized pair distance, k is Boltzmann's constant, T is the temperature, e is the elementary charge, and ϵ is the dielectric constant ($\epsilon = \epsilon_0\epsilon_r$).[7] The relative permittivity of the film, ϵ_r, was determined from capacitance measurement (Philips PM6303A automatic RCL meter).

The Onsager's model has been more extensively used for xerographic discharge (XD) data than for PC measurements. This is due to the influence of the charge carrier photogeneration efficiency, as well as the subsequent transport and trapping properties of the material.[12,22] Nevertheless, it has been observed that, taking into consideration the trap density of the material, the absolute quantum efficiency resulting from XD measurements is susceptible of comparison to the external photocurrent efficiency resulting from PC measurements.[22] PC measurements are completely adequate to compare samples with similar nature and different composition to optimize the different PVK(x)/TNF(y)-based sol−gel materials.

3. Results and Discussion

3.1. Photoconductive Characterization. PVK(12%)/TNF(6%)-based sol−gel materials were found to show a photosensitivity of 1.1×10^{-11} cm Ω^{-1} W^{-1} at an applied external electric field of $E \approx 14$ V μm^{-1}.[31,37] An increase from 0.7×10^{-11} to 1.1×10^{-11} cm Ω^{-1} W^{-1} at $E \approx 14$ V μm^{-1} in the S_{ph} was observed in PVK(12%)/TNF(6%)-based sol−gel photoconductive material as compared to the nonpolymerized sample NVC(12%)/TNF(6%)-based sol−gel material (before the UV irradiation).[31,37] This increase in S_{ph} is related to the favored transport of the charge carriers in the continuous medium obtained by the PVK chain. Besides, the silanol groups of the porous silica surface can be considered as impurities that induce effective holes trapping.[15]

In this work, the incorporation of the glycidoxypropyl groups in the silica surface provided a cage environment, which almost isolated the PVK network from the silica surface (and, hence, from its potential trapping centers), resulting in the enhancement of the charge carriers mobility. In addition, the PVK/TNF-based photoconductive sol−gel material shows better photocurrent signal stability after UV irradiation, e.g., the photocurrent signal was highly stable after 5 min in PVK/TNF-based photoconductive sol−gel materials, and it shows a ca. ±5% variation in NVC-based photoconductive sol−gel materials.

Modification of the PVK/SiO$_2$ Molar Ratios. The adequate balance between PVK and the supporting SiO_2 matrix allows a better photoconductive behavior of the PVK/TNF-based sol−gel materials to be achieved. Photosensitivity values from the PVK/TNF-based photoconductive sol−gel materials were similar to those obtained for other PVK-based materials (Table 1). This is the first indication of the unneeded use of massive PVK material as the host matrix in the preparation of photoconductive materials. Figure 2 shows the photosensitivity as a function of the applied electric field for a set of PVK(x)/TNF(y)-based sol−gel materials with different PVK contents, keeping constant the TNF content: e.g., $x = 3.6\%$, 7%, 12%, and 20% and $y = 0.21\%$.[37] It can be observed that the increase of PVK content up to 12% results in a better photosensitivity. Further increase of the PVK content results in a decrease of the photoconductivity (Table 2).

TABLE 1: S_{ph} Values[a] for Photoconductive Materials Prepared through Different Approaches for $E \geq 22$ V μm^{-1}

S_{ph} (cm/ΩW)	type of material	ref
3.38×10^{-10}	PVK(12%)/TNF(0.18%) sol−gel	*b*
10^{-12}	PVK/CdS or C_{60}-nanocrystal polymer composite	12
10^{-11}	full-functionalized polymer composite	16
10^{-14}	PVK/ECZ/TNF/chromophore polymer composite	22
10^{-14}	carbazole discrete units within a sol−gel matrix	28
10^{-10}	PVK/ECZ/C_{60}/chromophore polymer composite	36
10^{-10}	PVK/TNF/chromophore polymer composite	38
10^{-13}−10^{-12}	transition metal doped conjugated polymers	39
10^{-12}−10^{-11}	PVK:DCST or CEST Chromophore:BBP:C_{60}	40
10^{-13}	PM-1/PH-1 or PH-2/TNF molecular materials	41

[a] The value selected from PVK/TNF based sol−gel sample corresponds to a PVK(12%)/TNF(0.18) sample, where $x = 12\%$ stands for PVK/GPTMS molar ratio × 100 and $y = 0.18\%$ for TNF/PVK molar ratio × 100. [b] This work.

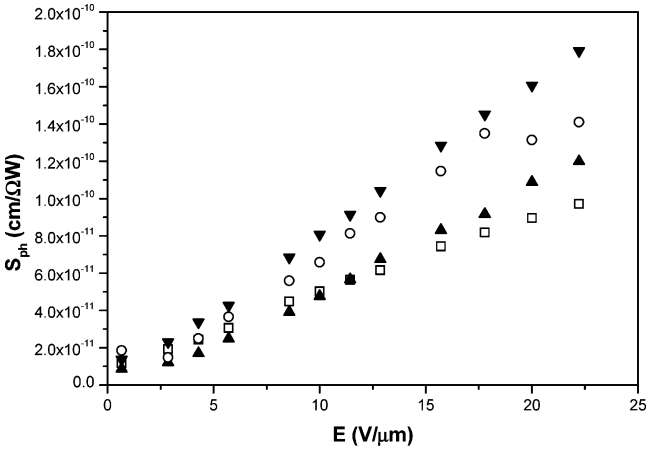

Figure 2. Photosensitivity curves (S_{ph}) as a function of the applied electric field, measured at 514 nm, for PVK(x)/TNF(y) samples, where y stands for TNF/PVK molar ratio × 100 ($y = 0.21\%$) and x for PVK/GPTMS molar ratio × 100 [$x = 3.6\%$ (▲), 7% (○), 12% (▼), and 20% (□)].

TABLE 2: Sample's Main Parameters[a] and r_0 and ϕ_0 Values Obtained from the Analysis of the Φ Experimental Data via Onsager's Model (Eq 3)

%PVK/ %TNF	αd	ϵ_r	$10^{-10}S_{ph}$ (cm /ΩW)	Φ	r_0 (Å)	ϕ_0
12/6	0.520	1.75	0.19	2.7×10^{-5}	40.24	9.0×10^{-4}
12/1	0.086	1.56	0.25	2.2×10^{-4}	43.35	0.007
12/0.5	0.046	1.42	0.66	1.1×10^{-3}	47.30	0.029
12/0.25	0.021	1.33	1.07	3.8×10^{-3}	51.05	0.078
12/0.21	0.018	1.32	1.79	8.1×10^{-3}	61.07	0.067
12/0.18	0.015	1.29	3.38	1.9×10^{-2}	66.10	0.120
12/0.1	0.012	1.29	1.42	1.0×10^{-2}	62.14	0.079
20/0.21	0.013	2.06	0.97	6.1×10^{-3}	39.79	0.114
7/0.21	0.024	1.26	1.41	5.0×10^{-3}	67.96	0.031
3.6/0.21	0.034	1.22	1.20	1.5×10^{-3}	64.26	0.011

[a] Absorption coefficient and thickness product, α*d*, dielectric constant, ϵ_r, photosensitivity, from eq 1, and experimentally obtained photogeneration efficiency, Φ, from eq 2 and at 514 nm. α*d* was measured at $\lambda = 514$ nm; S_{ph} was measured at $E \approx 22.2$ V μm^{-1}; Φ was obtained from eq 2 at $E = 20$ V μm^{-1}; and r_0 and ϕ_0 were determined from the best fit to the Onsager's model (eq 3).

It is worth to noting that the incorporation of just a 3.6% NVC in the initial solution stage (sample PVK(3.6%)/TNF(0.21%)) provides a material with good photosensitivity at low applied electric fields ($S_{ph} = 1.20 \times 10^{-10}$ cm Ω^{-1} W^{-1} at $E \approx 22$ V μm^{-1}).

Modification of the PVK/TNF Molar Ratios. The photosensitivity was increased by more than 1 order of magnitude when

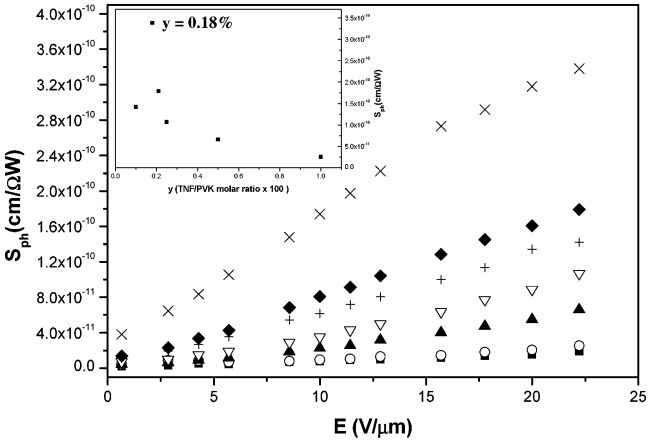

Figure 3. Photosensitivity curves (S_{ph} as a function of the applied electric field measured at 514 nm) for PVK(x)/TNF(y)-based sol−gel samples, where $x = 12\%$ and $y = 6\%$ (■), 1% (○), 0.5% (▲), 0.25% (▽), 0.21% (◆), 0.18% (×), and 0.1% (+). In the inset, photosensitivity evolution for PVK(x)/TNF(y)-based sol−gel samples, where $x = 12\%$ and $y = 6\%$, 1%, 0.5%, 0.25%, 0.21%, 0.18%, and 0.1%, at a fixed applied electric field ($E \approx 22$ V μm^{-1}) and at 514 nm is depicted.

the TNF content was decreased from 6% to 0.18% (Table 2 and Figure 3). To our knowledge, the photosensitivity of PVK-(12%)/TNF(0.18%)-based sol−gel material ($S_{ph} \approx 3.4 \times 10^{-10}$ cm Ω^{-1} W^{-1}, at ca. 22 V μm^{-1}, Table 2) is in range of the highest values ever reported for any PVK/TNF classical photoconductive material (Table 1). This photosensitivity enhancement at low TNF concentrations is related to a favored transport, rather than to a more efficient formation of CT complexes.

The low dark current level found in the PVK(12%)/TNF-(0.18%)-based sol−gel material ($J_{dark} \approx 10^{-13}$ A cm^{-2} without applied field and $J_{dark} \approx 10^{-9}$ A cm^{-2} for a low applied field of ca.10 V μm^{-1}) is also remarkable, since it is highly desirable for a photoconductor to exhibit no conductive activity under dark conditions.[12,42] In addition, the photoresponse observed without external electric field ($J_{ph}(E=0)$) is 2−5 times higher than the current signal under dark conditions and without external electric field ($J_{dark}(E=0)$) at an irradiance of 3 mW cm^{-2} for different samples (Figure 3). As in the case of organic photorefractive materials,[42] this behavior could be explained in terms of the generation of a weak gradient of photoexcited charge carriers across the sample. This weak gradient is a consequence of the fact that the light is mainly absorbed at the incoming surface of the PVK/TNF-based photoconductive sol−gel thin film, and this produces a weak electric field capable of transporting the charge carriers.

3.2. The Photocurrent Efficiency. Photocurrent efficiencies obtained from eq 2 for the PVK(x)/TNF(y)-based photoconductive sol−gel material for different PVK/TNF and PVK/GPTMS molar ratios (different x and y values) at $E = 20$ V μm^{-1} are shown in Table 3. As compared to a PVK/TNF classical polymeric material with the same TNF molar ratio (6%),[7] the lower Φ value obtained in the PVK/TNF-based sol−gel materials may be due to the fact that it is calculated from PC rather than from XD measurements. PC measurements are influenced by the differences between the contact working functions and the recombination and trapping processes.[22] Onsager's model is used to clarify if the origin of this behavior is a consequence of a less efficient photogeneration process. The Φ analysis via such a model was realized by fitting the Φ experimental data from eq 2 into eq 3, ignoring the irrelevant terms (i.e., recurrent terms corresponding to orders higher than the 56th in the series showed in eq 3 were not considered). Figure 4 shows the best Onsager's model fitting of the photocurrent efficiency experimental data for the PVK(12%)/TNF(0.18%)-based sol−gel material.

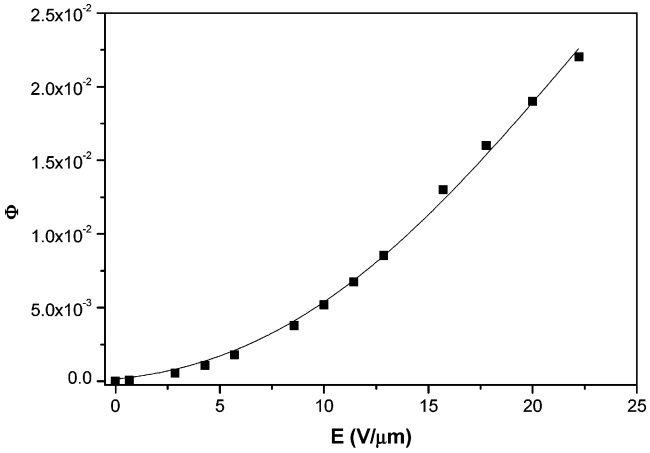

Figure 4. Fitting of the charge generation quantum efficiency experimentally obtained for the PVK(12%)/TNF(0.18%)-based sol−gel samples (■) to the Onsager's model (solid line).

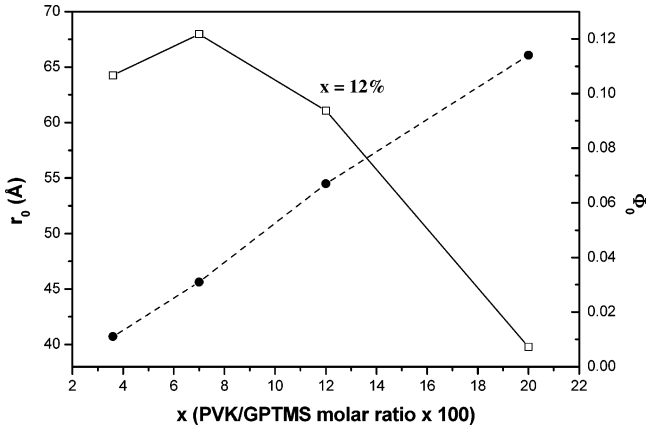

Figure 5. Evolution of Onsager's parameters as a function of the PVK content for several PVK(x)/TNF(0.21%)-based sol−gel samples: r_0 (open squares and straight line) and ϕ_0 (solid circles and dashed line).

TABLE 3: Onsager's Model Parameters (ϕ_0 and r_0) and Photocurrent Efficiency (Φ, at 20 V μm^{-1}) Experimentally Obtained for the PVK(12%)/TNF(6%) and PVK(12%)/TNF(0.18%)-Based Sol−Gel Materials Prepared in This Work and Those Reported for a Classical PVK/TNF Classical Polymeric Material[7]

sample	ϕ_0	r_0 (Å)	Φ
PVK(12%)/TNF(6%) polymer	2.3×10^{-1}	25.0	4.0×10^{-3}
PVK(12%)/TNF(6%) sol−gel	9.0×10^{-4}	40.2	2.7×10^{-5}
PVK(12%)/TNF(0.18%) sol−gel	1.1×10^{-1}	68.4	1.9×10^{-2}

The Onsager Analysis for Different PVK/SiO_2 Molar Ratios. PVK/TNF-based sol−gel samples with different PVK/SiO_2 molar ratios (different x values), and for a fixed TNF content ($y = 0.21\%$), were analyzed. The ϕ_0 (primary quantum yield) and r_0 (initial thermalized pair distance) values, obtained from the analysis of the experimental Φ, eq 2, through the employment of Onsager's model, eq 3, are shown in Table 2. The maximum Φ value, $\Phi = 8.1 \times 10^{-3}$ at ca. 22 V μm^{-1}, corresponds to the case in which ϕ_0 and r_0 are both high in the PVK(12%)/TNF(0.21%)-based sol−gel material. Figure 5 shows the r_0 and ϕ_0 tendencies for PVK/TNF-based sol−gel samples with a fixed amount of TNF ($y = 0.21\%$) and a changing PVK content. Increasing PVK concentration resulted in higher ϕ_0

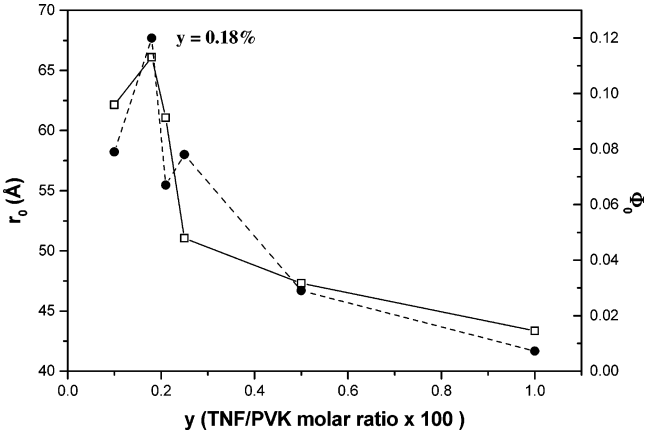

Figure 6. Evolution of Onsager's parameters as a function of the TNF content for several PVK(12%)/TNF(y)-based sol−gel samples: r_0 (open squares and straight line) and ϕ_0 (solid circles and dashed line).

values, since large amounts of PVK may induce the CT complex formation. Increasing PVK concentration also resulted in lower r_0 values due to the excess of PVK that includes undesirable potential traps, which favor the recombination processes. Thus, it seems to be clear that it is necessary to achieve a compromise in which ϕ_0 is large enough to have an important amount of charge carriers, but with r_0 large enough to avoid their recombination in the first steps of the transport process.

It can be observed that r_0 values do not follow the classical tendency reported for classical polymeric samples. For PVK/TNF-based sol−gel samples, large values of r_0 correspond to large Φ values under low electric-field conditions, due to a more hindered recombination of the thermalized pairs (Tables 2 and 3).[6] Such a behavior could be due to the use of the ϵ_r macroscopic value in Onsager's analysis. It was suggested that the macroscopic value of ϵ_r can be different from the local value, given the short dimensional range of the photogeneration process.[22] Taking this into account, the Φ experimental data of the PVK/TNF-based sol−gel materials were fitted to Onsager's model by using a different value for the dielectric constant than that experimentally measured, the macroscopic one, which was $\epsilon_r = 1.75$ for PVK(12%)/TNF(6%). The comparison of the results obtained in $\phi_0 = 7.8 \times 10^{-3}$ and $r_0 = 25.0$ Å in the PVK/TNF-based sol−gel sample, using a ϵ_r typical value in a PVK/TNF classical polymeric sample, $\epsilon_r = 2.30$ for PVK(12%)/TNF(6%), with the ϕ_0 and r_0 values in PVK/TNF classical polymeric samples (Table 3), shows that ϕ_0 still remains low for similar r_0 values. This indicates that the ϕ_0 value is strongly determined by the low value of the experimental Φ. Thus, ϕ_0 should somehow resemble not only the quantum efficiency of thermalized pair formation, but also the long-range recombination processes resulting from transport and trapping mechanisms. The behavior of ϕ_0 should be better understood by applying a higher electric field than that applied in this work.

Onsager Analysis for Different TNF Contents. PVK/TNF-based sol−gel samples with different PVK/TNF molar ratios (different y values) and for a fixed PVK content ($x = 12\%$) were analyzed. A 12% value was selected as the more appropriate PVK content, since it showed the highest S_{ph} and Φ values (Table 2). This situation corresponds to the simultaneous achievement of r_0 and ϕ_0 high values (Figure 5). ϕ_0 and r_0 results were obtained from the analysis of the experimental Φ with Onsager's model. By comparing samples with different TNF contents, it can be observed that r_0 follows the classical tendency reported for classical polymeric samples mentioned above (Table 2 and Figure 6).[6]

The decrease in the TNF content from 6% to 0.18% in the PVK/TNF-based photoconductive sol−gel materials shows a notorious improvement (close to 3 orders of magnitude) in the Φ value (Table 3), which is in good agreement with the improvement of S_{ph} discussed above. Whether or not such improvement is a consequence of a more efficient photogeneration process can be elucidated by the analysis of the Φ experimentally obtained via Onsager's analysis. ϕ_0 and r_0 results obtained for the sample with low TNF content resemble indeed a more efficient photogeneration process than that of samples with high TNF content. The ϕ_0 and r_0 values show an expected tendency: larger r_0 values inhibit recombination, resulting in an increase of Φ at the electric fields used in this work (Table 2). Nevertheless, the increase of ϕ_0 is remarkably large, even though the low concentration of TNF should not favor the CT complex formation. This behavior corroborates the influence of the trap density on the ϕ_0 value when obtained from PC measurements.

4. Conclusions

A highly photoconductive PVK/TNF-based sol−gel material is reported in this work. The photosensitivity achieved, $S_{ph} \approx 3.4 \times 10^{-10}$ cm Ω^{-1} W^{-1} at $E \approx 22$ V μm^{-1} for PVK(12%)/TNF(0.18%) sol−gel material, is in range of the highest values ever reported for any PVK/TNF classical photoconductive polymeric material. The PVK/TNF-based photoconductive sol−gel material shows better stability in the photocurrent signal after UV irradiation. The ϕ_0 and r_0 values obtained through the application of Onsager's model reveal a notorious improvement of the photocurrent generation process for low TNF contents. Photorefractive materials based on this highly photoconductive PVK/TNF-based sol−gel material show a notorious improvement of the response time. Given the low ϵ_r value of these materials, the use of PVK/TNF-based sol−gel materials as the photoconductive element of a hybrid photorefractive material shall also contribute to improve its photorefractive performance. The remarkably high value of the rate of increase of the photogeneration efficiency obtained for this sol−gel material, $\Phi(E \approx 20$ V μm$^{-1})/\Phi(E \approx 1$ V μm$^{-1}) \approx 250$, for PVK(12%)/TNF(0.18%), allows better performance of the sol−gel material at low external applied electric fields.

Acknowledgment. We thank the CICYT for research grants MAT 2005-05131-C02-01 and NAN2004-09317-C04-02. Gonzalo Ramos is also grateful to INTA for a Rafael Calvo Rodés fellowship. Dr. Francisco del Monte is acknowledged for valuable support.

References and Notes

(1) Zhang, Y.; Burzynski, R.; Ghosal, S.; Casstevens, M. K. *Adv. Mater.* **1996**, *8*, 111−125.

(2) Nalwa, H. S.; Miyata, S. In *Nonlinear organic molecules and polymers*; Nalwa, H. S., Miyata, S., Eds.; CRC Press: New York, 1997.

(3) (a) Batt, R. H.; Braun, C. L.; Horning, J. F. *J. Chem. Phys.* **1968**, *49*, 1967−1968. (b) Batt, R. H.; Braun, C. L.; Horning, J. F. *Appl. Opt. Suppl.* **1969**, *3*, 20.

(4) (a) Onsager, L. *J. Chem. Phys.* **1934**, *2*, 599−615. (b) Onsager, L. *Phys. Rev.* **1938**, *54*, 554−557.

(5) (a) Borsenberger, P. M.; Weiss, D. S. In *Organic Photoreceptors for Imaging Systems*; Thompson, B. J., Ed.; Marcel Dekker: New York, 1993. (b) Borsenberger, P. M.; Ateya, A. I. *J. Appl. Phys.* **1978**, *49*, 4035−4040.

(6) Pan, J.; Haarer, D. *Chem. Phys. Lett.* **2000**, *324*, 411−415.

(7) Melz, P. J. *J. Chem. Phys.* **1972**, *57*, 1694−1699.

(8) Pai, D. M. *J. Appl. Phys.* **1975**, *46*, 5122−5126

(9) Penwell, R. C.; Ganguly, B. N.; Smith, T. W. *J. Polym. Sci. Macromol. Rev.* **1978**, *13*, 63−160.

(10) (a) Urbach, J. C.; Meier, R. W. *Appl. Opt.* **1966**, *5*, 666−667. (b) Hariharan, P. In *Optical Holography. Principles, Techniques and Applications*; Cambridge University Press: Cambridge, UK, 1984.

(11) Carreño, F.; Martínez-Antón, J. C.; Bernabeu, E. *Thin Solid Films* **1995**, *263*, 206−212.

(12) (a) Winiarz, J. G.; Zhang, L.; Lal, M.; Friend, C. S.; Prasad, P. N. *Chem. Phys.* **1999**, *245*, 417−428. (b) Winiarz, J. G.; Zhang, L.; Lal, M.; Friend, C. S.; Prasad, P. N. *J. Am. Chem. Soc.* **1999**, *121*, 5287−5295. (c) Winiarz, J. G.; Zhang, L.; Park, J.; Prasad, P. N. *J. Phys. Chem. B* **2002**, *106*, 967−970.

(13) Moerner, W. E.; Silence, S. M. *Chem. Rev.* **1994**, *94*, 127−155.

(14) Bolink, H. J.; Krasnikov, V. V.; Malliaras, G. G.; Hadziioannou, G. *J. Phys. Chem.* **1996**, *100*, 16356−16360.

(15) Malliaras, G. G.; Krasnikov, V. V.; Bolink, H. J.; Hadziioannou, G. *Appl. Phys. Lett.* **1995**, *67*, 455−457.

(16) Gubler, U.; He, M.; Wright, D.; Roh, Y.; Twieg, R.; Moerner, W. E. *Adv. Mater.* **2002**, *14*, 313−317.

(17) West, K. S.; West, D. P.; Rahn, M. D.; Shakos, J. D.; Wade, F. A.; Khand, K.; King, T. A. *J. Appl. Phys.* **1998**, *84*, 5893−5899.

(18) Zilker, S. J. *ChemPhysChem.* **2000**, *1*, 72−87.

(19) Jung, J.; Glowacki, I.; Ulanski, J. *J. Chem. Phys.* **1999**, *110*, 7000−7007.

(20) Okamoto, K.; Nomura, T.; Park, S.; Ogino, K.; Sato, H. *Chem. Mater.* **1999**, *11*, 3279−3284.

(21) Würthner, F.; Wortmann, R.; Meerholz, K. *ChemPhysChem.* **2002**, *3*, 17−31.

(22) Däubler, T. K.; Bittner, R.; Meerholz, K.; Cimrová, V.; Neher, D. *Phys. Rev. B* **2000**, *61*, 13515−13527.

(23) Cottin, P.; Lessard, R. A.; Knystautas, É. J.; Roorda, S. *Nucl. Instrum. Methods Phys. Res., Sect. B* **1999**, *151*, 97−10021.

(24) Bittner, R.; Meerholz, K.; Stepanov, S. *Appl. Phys. Lett.* **1999**, *74*, 3723−3725.

(25) Safoula, G.; Bernede, J. C.; Touihri, S.; Alimi, K. *Eur. Polym. J.* **1998**, *34*, 1871−1876.

(26) Mercher, E.; Bräuchle, C.; Hörhold, H. H.; Hummelen, J. C.; Meerholz, K. *Phys. Chem. Chem. Phys.* **1999**, *1*, 1749−1756.

(27) (a) Zhang, Y.; Wada, T.; Sasabe, H. *J. Mater. Chem.* **1998**, *8*, 809−828. (b) Zhang, Y.; Wada, T.; Wang, L.; Sasabe, H. *Chem. Mater.* **1997**, *9*, 2798−2804.

(28) Darracq, B.; Chaput, F.; Lahlil, K.; Boilot, J. P.; Levy, Y.; Alain, V.; Ventelon, L.; Blanchard-Desce, M. *Opt. Mater.* **1998**, *9*, 265−270.

(29) Wang, Y.; Wang, X.; Li, J.; Mo, Z.; Zhao, X.; Jing, X.; Wang, F. *Adv. Mater.* **2001**, *13*, 1582−1585.

(30) Cheben, P.; del Monte, F.; Worsfold, D. J.; Carlsson, D. J.; Grover, C. P.; Mackenzie, J. D. *Nature* (*London*) **2000**, *408*, 64−67.

(31) Ramos, G.; Belenguer, T.; Bernabeu, E.; del Monte, F.; Levy, D. *J. Phys. Chem. B* **2003**, *107*, 110−112.

(32) Wang, S.; Yang, S.; Yang, C.; Li, Z.; Wang, J.; Ge, W. *J. Phys. Chem. B* **2000**, *104*, 11853−11858.

(33) Chen, Y.; Cai, R. F.; Xiao, L. X.; Huang, Z. E.; Pan, D. *J. Mater. Sci.* **1998**, *33*, 4633−4641.

(34) Ryzhii, V. *J. Appl. Phys.* **2001**, *89*, 5117−5123.

(35) Ostroverkhova, O.; Wright, D.; Gubler, U.; Moerner, W. E.; He, M.; Sastre-Santos, A.; Twieg, R. J. *Adv. Funct. Mater.* **2002**, *12*, 621−629.

(36) Hendrickx, E.; Zhang, Y.; Ferrio, K. B.; Herlocker, J. A.; Anderson, J.; Armstrong, N. R.; Mash, E. A.; Persoons, A. P.; Peyghambarian, N.; Kippelen, B. *J. Mater. Chem.* **1999**, *9*, 2251−2258.

(37) del Monte, F.; Ramos, G.; Belenguer, T.; Levy, D. Organic Holographic Materials and Applications; Meerholz, K., Ed. *Proc. SPIE−Int. Soc. Opt. Eng.* **2003**, *5216*, 91−98.

(38) Sandalphon, B.; Kippelen, N.; Peyghambarian, S.; Lyon, R.; Padias, A. B.; Hall, H. K., Jr. *Opt. Lett.* **1994**, *19*, 68−70.

(39) Wang, Q.; Yu, L. *J. Am. Chem. Soc.* **2000**, *122*, 11806−11811.

(40) Díaz-García, M. A.; Wright, D.; Casperson, J. D.; Smith, B.; Glazer, E.; Moerner, W. E. *Chem. Mater.* **1999**, *11*, 1784−1791.

(41) Choi, D. H.; Jun, W. G.; Oh, K. Y. In Organic Photorefractive and Photosensitive Materials for Holographic Applications; Meerholz, K., Ed. *Proc. SPIE−Int. Soc. Opt. Eng.* **2003**, *4802*, 146−153.

(42) Saleh, B. E. A.; Teich, M. C. In *Fundamental of Photonics*; Goodman, J. W., Ed.; John Wiley & Sons: New York, 1991.